Journal of Ambient Intelligence and Humanized Computing
https://doi.org/10.1007/s12652-018-0722-6

ORIGINAL RESEARCH

SPIRA: an automatic system to support lower limb injury assessment

Carlos Bailon[1] · Miguel Damas[1] · Hector Pomares[1] · Oresti Banos[2]

Received: 7 November 2017 / Accepted: 15 February 2018

Abstract
Lower limb injuries, especially those related to the knee joint, are some of the most common and severe injuries among sport practitioners. Consequently, a growing interest in the identification of subjects with high risk of injury has emerged during last years. One of the most commonly used injury risk factor is the measurement of joint angles during the execution of dynamic movements. To that end, techniques such as human motion capture and video analysis have been widely used. However, traditional procedures to measure joint angles present certain limitations, which makes this practice not practical in common clinical settings. This work presents SPIRA, a novel 2D video analysis system directed to support practitioners during the evaluation of joint angles in functional tests. The system employs an infrared camera to track retro-reflective markers attached to the patient's body joints and provide a real-time measurement of the joint angles in a cost-and-time-effective way. The information gathered by the sensor is processed and managed through a computer application that guides the expert during the execution of the tests and expedites the analysis of the results. In order to show the potential of the SPIRA system, a case study has been conducted, performing the analysis with the both the proposed system and a *gold-standard* in 2D offline video analysis. The results (ICC(ρ) = 0.996) reveal a good agreement between both tools and prove the reliability of SPIRA.

Keywords Injury risk · Lower limb · Joint angles · Marker tracking · Computer vision · Kinect · 2D video analysis

1 Introduction

Lower limb injuries are the most common injuries among sport practitioners and they are considered the main cause of sport practice disability. For that reason, this type of injuries has been subjected to many epidemiology studies during the last decades. According to van Gent et al. (2007), the overall incidence of these injuries rises up to 79.3%. In particular, knee joint complex injuries have been placed as the body regions with the higher injury risk (O'Connor et al. 2017; van Poppel et al. 2014; Hootman et al. 2007), which encompass more than the 20% of the lower limb injuries.

However, in order to correctly assess the impact of the knee joint injuries, it is necessary not only to analyze their incidence, but also to study the severity of their effects and their consequences to the affected individual. One of the most relevant and feared consequences is the sport time loss due to the injury recovery process which, specially in case of team sports, involves not only the physical harm to the individual but also the economic losses associated to its absence and treatment. The aforementioned studies show that the knee injuries carry the greatest time loss among lower limb injuries. The results presented in Booth and Orr (2017) sustain this affirmation and place the injuries affecting to knee ligaments as the ones which produce the highest number of absences in sport matches.

In particular, one of the most remarkable injuries of knee ligaments is the anterior cruciate ligament (ACL) tear. The ACL is one of a pair of fibrous connective tissues that connect the femur and tibia bones into the core of the knee joint. Although this disorder is less frequent than other ones, it stands out because it is associated with

✉ Carlos Bailon
cbailon@ugr.es

Miguel Damas
mdamas@ugr.es

Hector Pomares
hector@ugr.es

Oresti Banos
o.banoslegran@utwente.nl

[1] Department of Computer Architecture and Computer Technology, CITIC-UGR Research Center, University of Granada, Granada, Spain

[2] Telemedicine Group, University of Twente, Enschede, The Netherlands

Published online: 23 February 2018

potential long-term complications such as knee instability, meniscus tears or osteoarthritis (Acevedo et al. 2014). In most cases, this injury requires a surgery intervention and involves long rehabilitation periods, causing the cessation of the sport practice in more than the 11% of cases (Feller and Webster 2013; Hewett et al. 2013). It is also remarkable that the return to sport rate within two years is lower than 50%.

Moreover, this kind of serious sport injuries have become a public health concern due to the high financial costs of the surgery and rehabilitation process involved. According to Mather et al. (2013), in the long term, the mean lifetime cost to society for a patient following an ACL rehabilitation program is $88.538. The high cost of a full rehabilitation program makes this treatment unaffordable to many injured individuals, primarily in cost-constrained healthcare environments. However, it is known that accomplishing a prevention program in time can lead to a quantifiable reduction in the injury risk with a significant decrease of the treatment cost. For example, ACL injury risk can be reduced up to 52% in females and 85% in males (Kato et al. 2008).

In the light of the high impact and the aforementioned consequences of lower limb injuries such as the ACL tears, it becomes clear the relevance of identifying those subjects with a high risk of suffering injuries, in order to prevent the appearance of future injuries. To that end, the development of efficient screening, testing and assessment tools to support the injury risk evaluation has become an extremely important issue for healthcare professionals. Traditional injury risk assessment procedures can be improved by introducing digital technologies, which enable the automation of those practices, thus increasing the precision and reducing the time invested by experts during the evaluations and the analysis of the results. In fact, during the last years, the use of digital devices and software in healthcare procedures has become increasingly popular and widely used due to the constant technological improvement and the development of new devices and sensors. Some of the most important examples of its application are the rehabilitation support systems, which help the experts to precisely monitor the evolution of a patient during rehabilitation exercises through the information registered by multiple sensors (Banos et al. 2015; Bort-Roig et al. 2014; Davoody and Hagglund 2016).

Taking into consideration the challenges of injury risk assessment and the benefits of using digital technologies during the performance of the evaluations, this work presents SPIRA, a novel system to support practitioners during the assessment of a patient lower limb injury risk, substantially reducing the time investment for this task. The paper is structured as follows. Section 2 provides a description of the methodology of injury risk assessment and the main existing techniques for evaluation. The proposed SPIRA system is described in Sect. 3. In order to validate the system, a case study is presented in Sect. 4. Finally, the conclusions and remarks are summarized in Sect. 5.

2 Lower limb injury risk assessment

The first step when assessing the injury risk is the identification of the mechanism of injury, i.e. how the injury occurs. According to some researches (Booth and Orr 2017; Acevedo et al. 2014), the severity of the lower limb injuries received via non-contact mechanisms, particularly in knee and ankle, is much greater than those with contact mechanisms. Moreover, non-contact injuries affect predominantly to ligaments and tendons, which typically require lengthy rehabilitation processes. For that reason, in this work we will focus on studying the injuries produced in this way. Non-contact mechanisms refer to the injuries suffered when executing a specific movement that leads to a damage of the body, without involving any impact with an external element. In order to identify subjects with a high risk of suffering non-contact injuries, a widely used approach is to reproduce the movements that provoke the injury in a clinical setting, without risk of harm, and measure selected features of the movement which are related to the injury, known as injury risk factors. The analysis of these measurements can help to identify the high injury risk subjects. The exercises which reproduce the aforementioned movements are called functional tests.

Among the non-contact mechanisms of injury, one of the most commonly described, specially for knee injuries, is the unilateral landing from a jump. This involves landing with the hip extended and the knee in valgus position, also with internal rotation of the tibia and a pronated foot—the so called "position of no return"—(Hewett et al. 2005; Hewett and Myer 2011). This position, depicted on Fig. 1, produces a high knee abduction moment, resulting on the knee collapse.

Due to the relevance of the knee abduction when a knee injury occurs, the dynamic evaluation of the knee alignment appears as a useful injury risk factor to be evaluated during functional tests, in order to identify excessive knee valgus and landing abnormalities. Towards giving a quantitative measurement of the knee alignment, Wilson et al. introduced the Frontal Plane Projection Angle (FPPA) (Willson et al. 2006). It consists in the projection of the knee angle over the frontal body plane (Fig. 2). Many subsequent researches have demonstrated that the FPPA measured during functional tasks has a strong relationship with severe knee injuries as ACL injuries and Patellofemoral Pain Syndrome (PFPS), establishing the FPPA measurement as one of the primary predictors of these injuries (Willson and Davis 2008; Herrington and Munro 2010; Herrington 2014; Stickler et al. 2015). Some

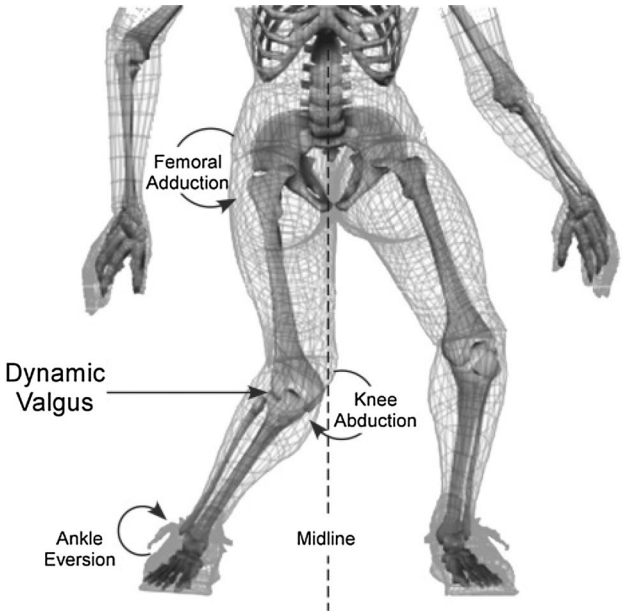

Fig. 1 Characteristic motions of the dynamic valgus at the "position of no return" (Hewett et al. 2005)

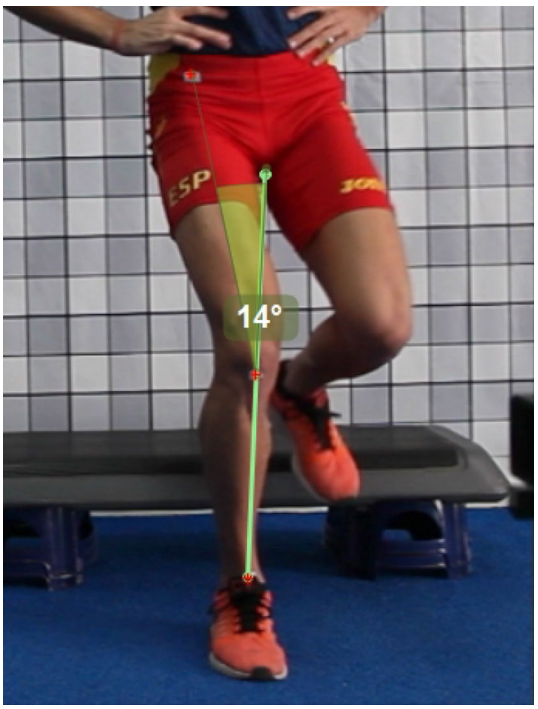

Fig. 2 Frontal plane projection angle (FPPA) (Bailon et al. 2017)

of the most interesting functional tasks to perform are the single leg landings (SLL) (Herrington and Munro 2010) and the single leg squats (SLS) (Willson and Davis 2008), as they involve unilateral movements and jump landings.

To measure the angles of the lower limb joints, including the FPPA, the most commonly used method is the video analysis. A range of retro-reflective markers are placed on the subject's body joints and the movements are captured by a computer vision system, usually composed by one or more color or infrared cameras. The system tracks the position of each marker over time, thus constructing the trajectory of each body joint, allowing us to represent the whole body movement (Vicon Motion Systems Ltd. 2002). Within this context we can distinguish between 3D and 2D motion capture. For the first case, the subject is surrounded by a set of calibrated an synchronized cameras which acquire 2D coordinates of each marker and, at the end, compose a precise 3D trajectory of each subject's joint by blending all the tracks. Powerful 3D marker-based motion tracking video systems are available, such as Vicon cameras (Vicon Motion Systems Ltd. 2017) or Optotrak system (Northern Digital Inc. 2017), both *gold-standards* in biomechanical analysis. However, despite their reliability and accuracy, its use requires large financial and spatial resources, since several expensive cameras are needed, forcing the experts to perform the analyses into a large and specifically equipped room (Willson and Davis 2008), making this technique not practical for most clinical settings and not affordable for most clinics.

Due to the aforementioned reasons, the 2D offline video analysis techniques have proliferated in an attempt of dealing with the amount of resources required by 3D video systems. 2D motion capture systems make use of just one camera, restricting the trajectories to one plane but employing less expensive, portable and easy-to-use equipment, which makes this technique more useful when capturing a specific angle. Many studies have introduced 2D video analysis in a variety of functional tests and have contrasted its validity against the existing 3D techniques (DiCesare et al. 2014; Wyndow et al. 2016; Munro 2013; Munro et al. 2012). These researches also show the reliability of 2D techniques when assessing knee injury risk, establish measurement error values for this type of analysis and emphasize the need for further investigation on these screening tools.

This type of analysis is performed as follows: the subject's movement is captured by a digital video camera and the video sequences are then introduced in a specific software, which allows the user to play the recordings in slow motion and freeze them at the desired frame. Afterwards the user identifies the joints' markers on the frozen frame and place lines connecting them, thus performing an estimation of the angle subtended by those lines. Even though this approach overcomes the resource limitations of the 3D video analysis in an effective and extremely simple way, the offline analysis has a potential limitation: the time consumption. Because of the offline analysis phase introduced, it demands a huge time investment, specially when evaluating multiple subjects. In addition, human-made errors are increased due

to correct video freezing and marker positioning. It is also worth considering the results obtained in Willson and Davis (2008); Munro et al. (2012), which affirm that 2D angle estimations as FPPA reflect 23–30% of the variance of 3D rotations. Nevertheless, although 2D analysis is not a substitute for 3D measurements, the previously mentioned studies also proved it to be useful for screening lower limb angles and identifying high injury risk subjects. One widely known 2D analysis software is *Kinovea* (Kinovea Association 2017), an open-source tool considered as the *gold-standard* of this technique.

3 SPIRA: a novel system for lower limb injury risk assessment

Taking into account the limitations of body angle measuring techniques and in an attempt to relate them with the lower limb injury risk, this work presents SPIRA, an innovative system to support practitioners during lower limb injury risk assessment procedures. The system uses an infrared camera to track retro-reflective markers attached to the body joints, computes the desired angle value from the markers' relative position and provides real-time information of their value. All the information gathered during the execution of the functional tests is seamlessly transmitted to a computer application with an intuitive user interface aimed at supporting and simplifying the expert's routine, helping to mitigate human errors and expedite the analysis of the results. In this context, the system uses a single-camera solution (thus removing the spatial and financial needs of 3D video analysis) and avoids the need of offline analysis, resulting on a cost-and-time-effective solution. In the following, the key features of the SPIRA system are thoroughly described.

3.1 System description

The main function of SPIRA is to track the retro-reflective markers attached to the patient's body joints and compute the angles subtended by them. To that end, the system is composed by three key elements. The first one is the set of markers. They are made of retro-reflective material so that they can be easily distinguished by an infrared sensor and avoid problems with the viewpoint of the camera, since the light is reflected in the same direction of the source. The markers' shape is not restricted, provided that their size is small enough to identify the exact location of the joint. In this work, we have used pieces of retro-reflective tape. In order to get a reliable value of the joint angles, the markers must be placed by an expert on the anatomic points that correspond to the exact location of the joints. For specific joints, a correction factor may be applied to the marker position in order to obtain the exact joint center. For the FPPA case, the hip joint center (HJC) was obtained using the approach described in Bell et al. (1989): the HJC is 30% distal, 14% medial and 22% posterior to the ASIS (marker placement), expresed as a percentage of the distance between the right and left ASIS.

The second key element is the infrared (IR) camera, whose role is to capture IR video frames and track the markers. The choice of an IR camera instead of a color one is based on the operating principle of the IR sensors: an emitter sends an IR light pattern to the scene, which is reflected and captured by a receiver. Depending on the distance, shape and material of the object where the light is reflected, the intensity of the pattern captured by the receiver will be different. In particular, retro-reflective elements reflect almost all the light sent, so its intensity value is extremely high. That is how the markers are identified. SPIRA is able to work with any IR camera with the appropriate pre-processing stage; however, for the present work, the system has been designed to operate on the infrared data provided by the Microsoft's Kinect V2 sensor (Microsoft 2014b), because of its easiness of use, quick development stage and low cost, in contrast to other high-end cameras. The IR camera included in the device is composed by a CMOS camera and three IR emitters. Its operation principle is the Time-of-Flight (ToF) approach, which works emitting a point cloud, in contrast to structured-light sensors (Sarbolandi et al. 2015; Li 2014).

The last element is a computer application that acquires and processes the information sent by the camera on-the-fly, computing the desired angle values and storing the results into a database. The aim of the application is to provide a framework to support and guide the expert over the execution of the functional tests, and a real-time visualization of the process and its results.

3.2 Marker tracking algorithm

In this section we describe the main functionality of the computer application, the reflective marker tracking. The developed algorithm has been implemented in the back-end layer of the application and encompasses the whole data processing from the acquisition of the camera's IR image to the computing of the desired angle. Figure 3 outlines the main steps of the algorithm, which will be thoroughly described in the following paragraphs. This process is repeated for each video frame arrived.

Image acquisition The first step of the algorithm is the acquisition, pre-processing and representation of the image. Kinect V2 sensor has a sampling rate of 30 Hz, its resolution is 512×424 pixels and codifies the IR intensity value of each pixel in 16 bits. This sampling rate has been proved to be enough to properly gather joint position data during functional tests (Müller et al. 2017). Therefore, each second it sends 30 video frames to the application,

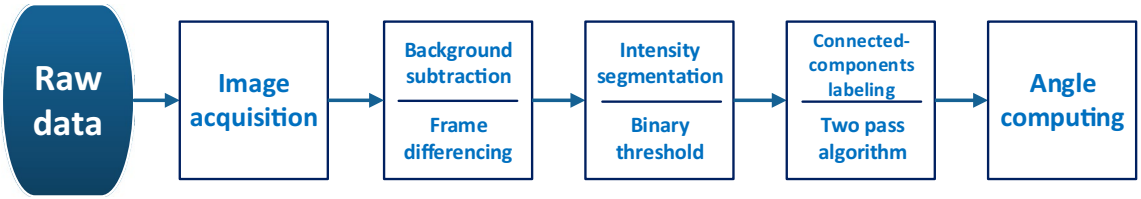

Fig. 3 Marker tracking algorithm

each one composed by a 512 × 424 array with a 16-bit value for each pixel, along with the frame metadata. Once the array has been received, we apply a normalization stage in order to scale the intensity value to the range [0, 1]. To achieve this, we use the *min–max normalization* technique (Patro and Sahu 2015). It applies a linear transformation to the original data, preserving the relationships among them. Equation (1) shows the procedure of a generalized min–max normalization stage, being $X \in [X_{min}, X_{max}]$ the original intensity value and $X' \in [X'_{min}, X'_{max}]$ the normalized value. In this specific case, $X'_{min} = 0$ and $X'_{max} = 1$.

$$X' = \frac{X - X_{min}}{X_{max} - X_{min}}(X'_{max} - X'_{min}) + X'_{min} \tag{1}$$

Figure 4a shows the image acquired after the normalization stage. It is worth noting the high infrared intensity of the markers.

Background subtraction Once the image has been normalized, we need to select the region of interest where the reflective markers are placed: the patients body. By focusing the search into this region, we reduce the computational load of the algorithm and ensure that any unintended reflective element in the scene is not wrongly detected as a marker. The approach followed to achieve this objective is the background subtraction, which consists in splitting the image into two layers, foreground (body) and background (rest of the image), and removing the second one. A wide range of techniques can be found in literature for background subtraction (Piccardi 2004), from simple thresholding to more complex background modeling using Gaussian probability density functions.

The injury risk assessment analyses are designed to be performed in a clinical setting, only to one patient at once. Therefore, the background is expected to be static during the whole process. For that reason, in this work we have opted for using a simple approach based on *frame differencing* (Bouwmans et al. 2015). The procedure is the following: at the beginning of the evaluation, before the patient positions into the camera field of view, a calibration stage is run, in which a reference image of the background is taken. Then, each time a new frame arrives, the intensity difference between the current frame and the background reference is computed. Those pixels whose intensity difference exceeds a threshold are considered foreground pixels, as shown in Eq. (2), where $I(x, y, t)$ denotes the intensity value of a pixel of a frame taken at time t and $B(x, y)$ denotes the intensity value of the same pixel on the background reference frame.

$$|I(x, y, t) - B(x, y)| > Threshold \tag{2}$$

The result of this stage is a binary image where the foreground pixels are set to 1. This simple approach reduces the resource consumption when compared to background modeling techniques, and the results yielded cover the needs of the current application. However, since the final image may have noise, within this stage we apply a Gaussian filter in order to blurry the edges and contours of the detected foreground, in a process known as *Gaussian smoothing* (Szeliski 2011). Finally, the foreground binary image (Fig. 4b) is applied as a mask for the next steps of the algorithm.

Intensity segmentation After selecting the region of interest for the marker detection, we need to select those pixels which belong to reflective markers. As it was mentioned in Sect. 3.1, the intensity value of these pixels is substantially higher than the rest of pixels of the image, so the segmentation of the markers is quite straightforward. In this work, we have applied a *binary threshold* or high pass filter, a widely used approach in image processing (Guerra-Filho 2005). For each frame, and after applying the previous step, every foreground pixel is compared to a selected intensity threshold. If the intensity value of the pixel exceeds the threshold is considered to be reflective, and hence, part of a marker. The result is a new binary image (Fig. 4c) where only the reflective pixels are set to 1. This image is also applied as a new mask for the last steps.

Connected-component labeling At this point, we have an image with all reflective pixels identified, but we do not know yet which group of pixels shapes each marker. For that reason, the this step aims to identify to which marker belongs each pixel, merging similar regions together and enumerating them. This task has been addressed in some motion capture works. One possible approach (Olugbara et al. 2015) could be running a clustering algorithm to differentiate the groups of pixels. However, when the relative distance between two markers is very short, some pixels of

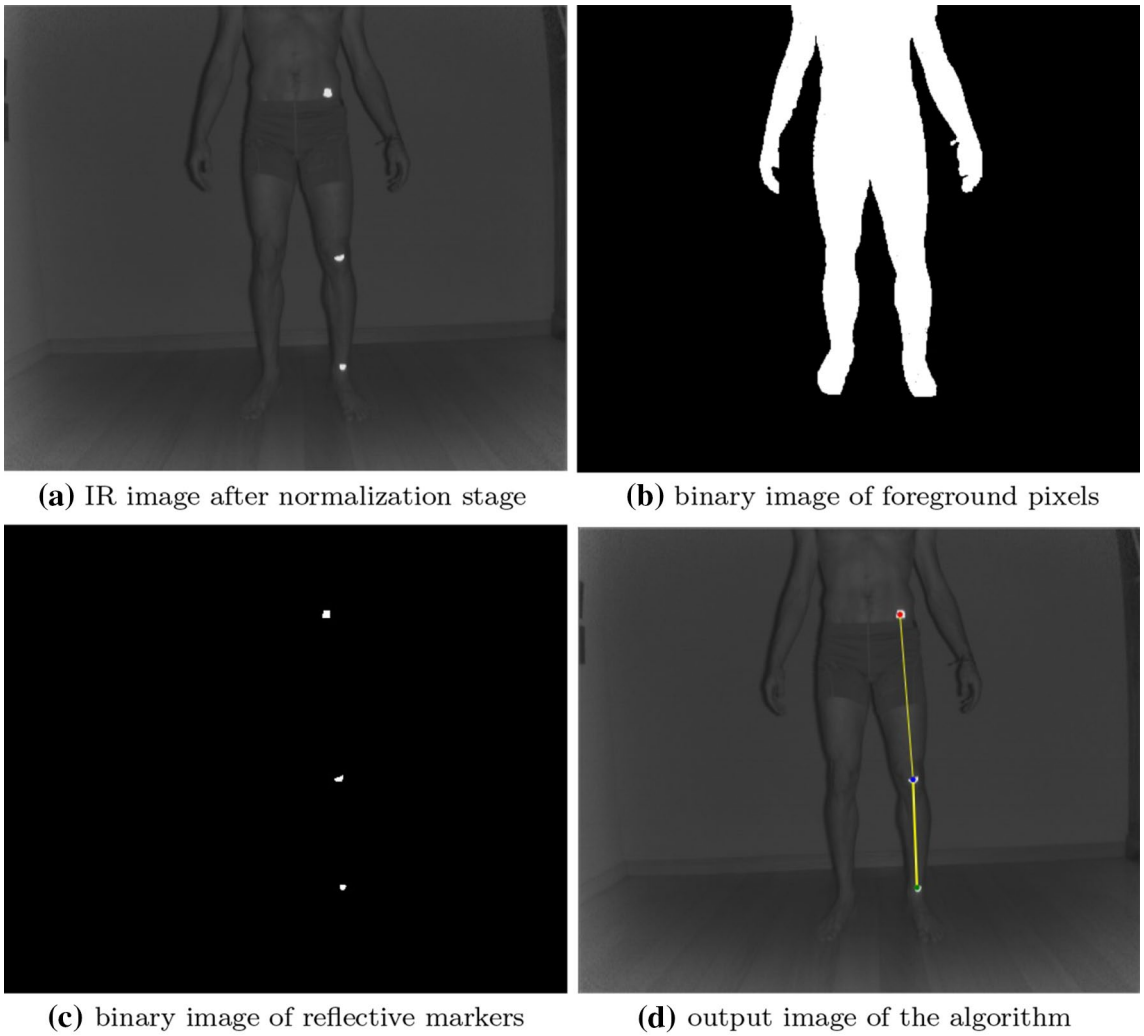

Fig. 4 Output images of the main steps of the algorithm

a marker could be wrongly assigned to an incorrect cluster, leading to detection errors. For that reason, other authors (Guerra-Filho 2005) make an algorithmic application of graph theory called *connected-component labeling*. The objective is to identify subsets of connected components (group of pixels) and assign them a unique label based on a given heuristic.

In this work, the approach used has been the *two-pass algorithm* (Shapiro and Stockman 2002), an iterative algorithm composed by two steps, which is outlined in Algorithm 1. The algorithm starts from the binary image generated by the intensity segmentation stage, where reflective pixels are set to 1 and the rest to 0. In each step, the algorithm iterates through each pixel of the image by columns and then by rows. In the following, both steps are described:

1. *Assignation* For each pixel that is not part of the background, the algorithm checks the neighbors which are labeled and assigns their label to the current pixel. If the neighbors have different labels, the algorithm stores the equivalence among them in a union-find structure (used in the second step), and assigns the smallest one among them to the current pixel. If there are no labeled neighbors, the label assigned to the current pixel is the next available number. After this pass, we get an image labeled with primary labels, probably including multiple labels for connected regions.
2. *Aggregation* The aim of this step is to merge the connected regions in a unique label. It performs another iteration over the whole image and, for every pixel, searches its label into the union-find structure and relabels the pixel with the lowest equivalent label.

The output of the algorithm is an image with every reflective pixel labeled. As every connected region has its

pixels equally labeled, now we can identify which group of pixels belong to each marker.

Algorithm 1 TwoPass(image)

```
nextLabel = 1
linked = [ ]
labels = [ ]
function FIRST-PASS(image)                                  ▷ Assignation
    for each row in image do
        for each col in row do
            if image[row][col] ≠ background then
                neighbors = connected elements
                if neighbors ≠ empty then
                    L = neighbors labels
                    labels[row][col] = min(L)
                    for each label in L do
                        linked[label] = union(linked[label],L)
                else
                    linked[nextLabel] = nextLabel
                    labels[row][col] = nextLabel
                    nextLabel += 1
function SECOND-PASS(image)                                 ▷ Aggregation
    for each row in image do
        for each col in row do
            if image[row][col] ≠ background then
                labels[row][col] = find(linked[labels[row][col]])
```

Angle computing This is the last step of the algorithm. First of all, it is necessary to determine the exact location of every marker. In order to avoid shape and size restrictions for the markers, we compute their coordinates as the centroid of each labeled group of pixels. After that, any desired angle can be computed based on their relative position. Figure 4d shows the identification of the markers and the connections among them.

3.3 Application description

One of the main aims of SPIRA is to give experts a user friendly interface to guide them during the execution of functional tests and expedite the visualization and analysis of the results. This objective is achieved through the computer application designed to manage the marker tracking algorithm. In the following, the main features of the application are described. For the first time use, and each time a new patient will be evaluated, the expert has to create the patient's profile in the system database. A new patient registry needs to be filled with personal information such as name, age, height, width, gender and relevant health conditions. At this point, an unambiguous ID number is assigned to the patient, which will be his identification code. Existing profiles can also be edited or deleted.

Once the profiles have been added to the database, the user can perform a variety of functional tests to measure different body angles during the execution of specific movements. When selecting a test, the specialist is redirected to a new window that enables the visualization and control of the test procedure. Figure 5 depicts the main screen of the Single Leg Landing (SLL) test, which measures the FPPA. The window is divided into three sections. The left one shows the visualization of the camera image, where the markers of the desired joints are tagged with a color point (after obtaining its coordinates with the algorithm described in Sect. 3.2), and connected with thin lines, representing the bones between the joints. In the aforementioned figure, the hip, knee and ankle markers are represented with color

Fig. 5 Single leg landing test window

circles, respectively. The central section is the control panel, which contains multiple buttons for the test management. First of all the expert has to select the patient's profile from a drop-down list, and select the leg which will be evaluated. Then, the test can be started by clicking on the *Start* button and ended clicking on the *Stop* button. During the execution of the test, the real-time angle value is shown below these buttons. The expert can perform all test trials s/he want to, by clicking on the *New Trial* button. All the results of past trials can be visualized by selecting them from another drop-down list, which is only enabled when a trial is not running. Finally, when the test is finished, if the *Save Results* button is clicked, it shows a pop-up dialog which allows the expert to select the trials that s/he want to save. The right area of the window shows a data chart that displays a real-time graph of the angle evolution during the test execution. It allows the expert to easily visualize the angle fluctuations during the test.

After performing the tests, the expert can navigate to another window where all patients' historical data are displayed on a table (Fig. 6). Through a drop-down list, the expert can select a particular test and/or user, and visualize the results only for this specific combination. The information of the table is complemented with a chart that displays graphically the evolution of a specific test and user over time. This allows the expert to visualize this evolution graphically and design prevention programs for those users whose risk of injury is growing.

3.4 Application implementation

The application has been developed within the .NET framework (Microsoft 2017a), due to its great integration with the Kinect SDK. The application high-level architecture is depicted in Fig. 7.

The implementation is split into a back-end layer, where the marker tracking algorithm, application functionalities, data storage and sensor communication has been developed; and a front-end layer, which contains the user interface (UI) design. The UI design and the communication between back-end and front-end is managed through the Windows Presentation Foundation (WPF) API (Microsoft 2017b). Each window of the application is designed in the front-end layer through a wide range of pre-defined UI elements called *controls*. This layer is written using XAML (Microsoft 2017c), a declarative markup language based on XML. Then, each window has its own back-end code, written in C#, which implements all the interactions and functionalities. The WPF API

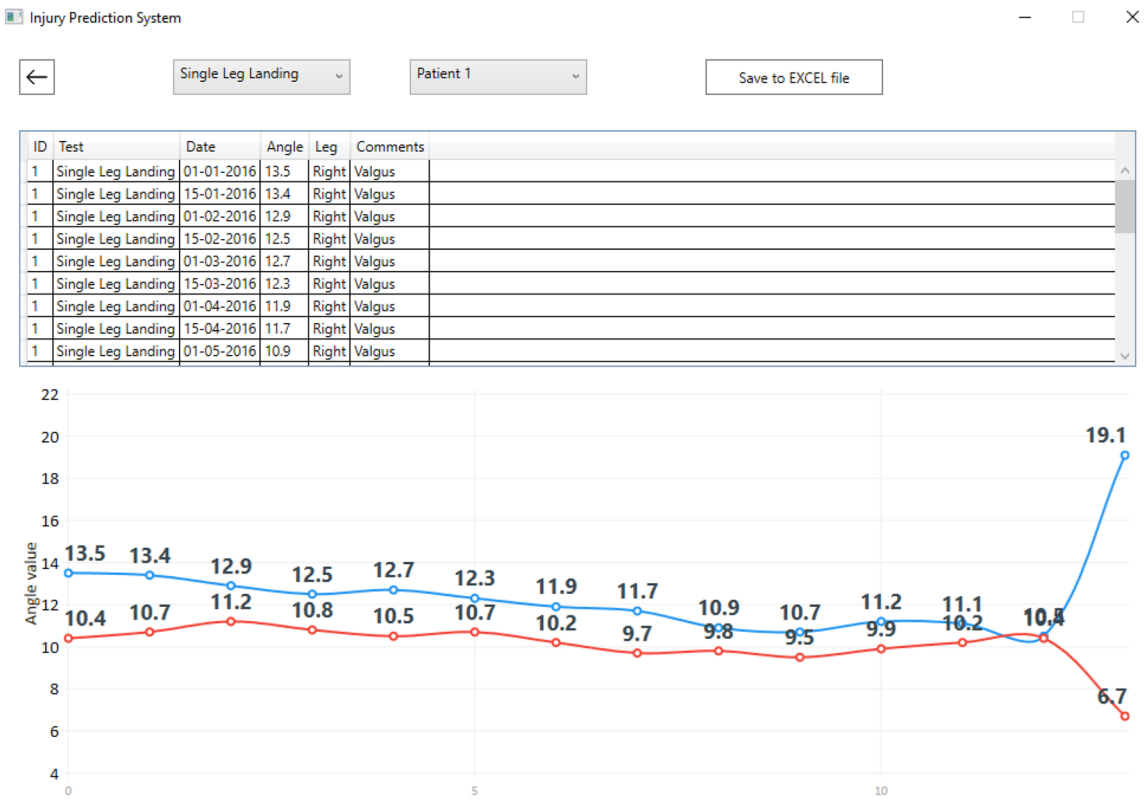

Fig. 6 Historical data analysis window

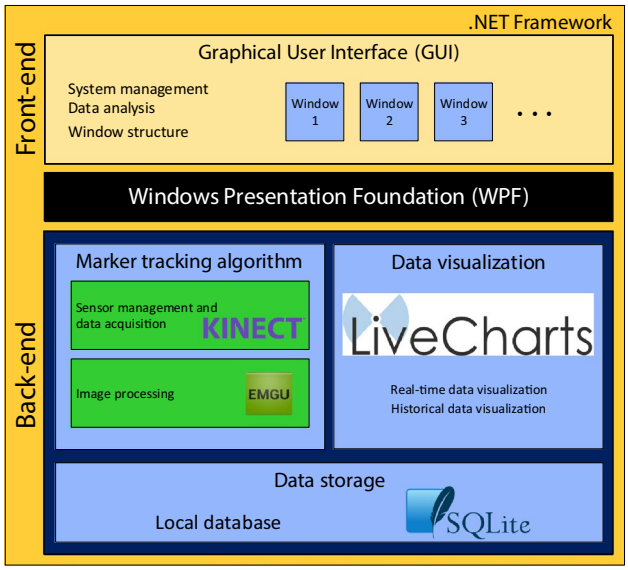

Fig. 7 High-level architecture of SPIRA

treats every window of the application as an object, with its own properties and connections with other windows, and every UI control as another object within the window.

The key feature of the SPIRA system is the marker tracking algorithm. This functionality has been developed on the back-end layer of each test window. For the management of the sensor and the raw data acquisition, Kinect API (Microsoft 2014a) has been used. It provides a great structure of objects and functions to work with the different data sources of the Kinect sensor. In combination with it, the algorithm has been implemented using the EmguCV library (EmguCV 2017), a cross-platform .NET wrapper of OpenCV image processing library.

The system storage functionality relies on a local SQLite database (SQLite 2017) deployed within the user's computer. It splits the information into two tables, one with the personal information of the patients introduced when their profile is created, and the other with the results of each test performed and saved. Both tables are only related through the patient's ID number, in order to keep patients' privacy safe. The database has been deployed locally, in detriment of client/server engines, since it adjusts better to the characteristics of our project (small amount of data stored, non-concurrent queries).

The application also provides a real-time graphical representation of the angle evolution during the execution of a test, as well as of the historical test results. This feature has been implemented using the open-source LiveCharts library (LiveCharts 2017).

4 Validation

In order to check the reliability of the SPIRA system it has been validated against Kinovea software, a *gold-standard* in 2D offline video analysis whose use in physical therapy is very extended (Damsted et al. 2015; Moral-Muñoz et al. 2015). This software allows the user to analyze previously recorded video sequences, running them at slow motion and freezing the video at the desired frame, where the user can place manually lines and markers to identify the body joints and compute an estimation of the angles between them. The functional test chosen to perform the validation study has been the Single Leg Landing (SLL) Test, due to its promptness and simplicity, saving time to the experts and making it easier for the patients to understand the procedure. This test simulates a unilateral landing from an elevated platform, and the FPPA is measured during the whole process, focusing on the highest value obtained, which represents the maximum knee abduction, a key injury risk factor (see Sect. 2).

For the FPPA measurement, the hip, knee and ankle joints have to be identified, so the expert have to strictly place three retro-reflective markers on the anatomic points described in Willson et al. (2006): (1) anterior superior iliac spine (ASIS), (2) middle of the tibiofemoral joint and (3) middle of the ankle mortise. The test has been conducted with the methodology proposed in Herrington and Munro (2010): the subject has to step-off a 30-cm-high bench landing with the opposite leg onto a mark positioned 30 cm from the bench, and hold the position for at least 2 s. During the test, the subject has to keep the hands on their hips and ensure that the contralateral leg makes no contact with any other object or surface. The sensor is placed at the subject's knee level, 2 m away from the landing target and aligned perpendicular to the frontal plane. It is recommended to perform various landings with each leg in order to remove wrongly executed landings.

Previous researches have demonstrated that both, structured-light and ToF sensors, can suffer from ambient background light interferences. It can either lead to over-saturation when exposure times are too long in relation to the object's distance, or cause problems in detecting the light pattern due to reflectivity (Sarbolandi et al. 2015). For that reason, although Kinect sensor includes a band-pass filter which suppresses background light, this validation has been performed in a clinical setting where light conditions are controlled to avoid the aforementioned problems.

To perform the study, ten healthy volunteers, five males and five females (mean age 25.8, SD 5.6 years) were recruited to be evaluated in a SLL test by two external physical therapists. The evaluation was performed in a

Sport Center at University of Granada, using both SPIRA and Kinovea software. All the subjects practiced sport at least twice a week and were not injured at the moment of the evaluation. The execution of the test was recorded simultaneously with the Kinect sensor and with a digital color video camera, one placed above the other with the minimum possible lens displacement. Before performing the evaluation, the subjects were informed about the research aims and the SLL was explained. Each of them performed a experimental trial in order to become familiar with the required movement. After that, each participant performed three test attempts with a resting time of 30 s. The SPIRA system obtained the FPPA value automatically, while the digital video camera recordings had to be introduced in a computer and analyzed offline with Kinovea software by the same physical therapists that conducted the study. The final result of each test is the mean FPPA of the three attempts performed by the subject.

The results are collected in Table 1. As it can be observed, the results obtained through both methods are generally in line, which reflects the utility of SPIRA. To support this observation, a formal statistical analysis has been performed, calculating the intraclass correlation coefficient (ICC)(ρ) (Bland and Altman 1990), a statistic widely used in the clinical domain to evaluate the agreement among two different instruments. The results have been extracted using

Table 1 Validation study results. Angle values are expressed in degrees (°)

Patient ID	1	2	3	4	5	6	7	8	9	10
Age	26	22	21	23	36	18	31	25	32	24
Trial 1 (S)	12.4	13.5	14.9	14.1	18.7	20.2	10.8	9.7	13.4	17.1
Trial 1 (K)	12	14	15	14	18	21	12	9	13	17
Trial 2 (S)	17.6	21.4	12.8	15.1	15.8	16.2	6.7	12.6	15	21
Trial 2 (K)	18	22	14	16	16	17	5	12	15	21
Trial 3 (S)	18.7	16.3	9.6	23.3	18.2	17.4	8.5	8.7	12.4	18.7
Trial 3 (K)	19	16	10	23	18	17	8	9	12	19
Average (S)	16.2	17.1	12.4	17.5	17.6	17.9	8.7	10.3	13.6	18.9
Average (K)	16.3	17.3	13	17.7	17.3	18.3	8.3	10	13.3	19
Absolute error	0.1	0.2	0.6	0.2	0.3	0.4	0.4	0.3	0.3	0.1
Relative error	0.006	0.012	0.046	0.011	0.017	0.022	0.048	0.030	0.023	0.005

K Kinovea, *S* SPIRA

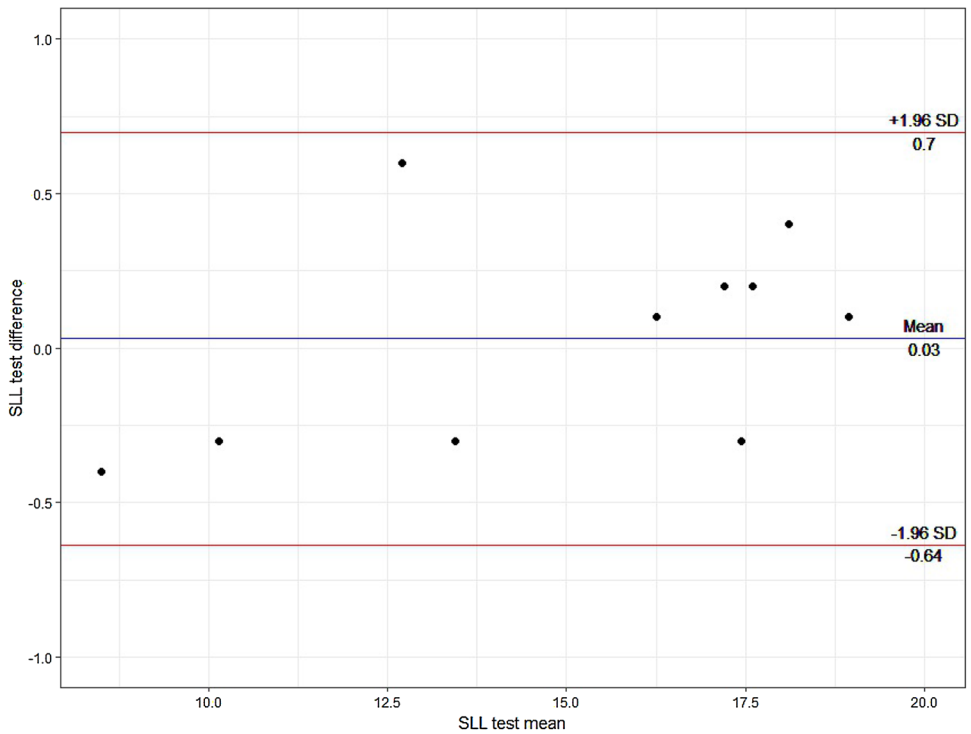

Fig. 8 Agreement between 2D offline video analysis and SPIRA through a Bland–Altmann plot. The mean of differences ($\bar{x}$) is represented by a blue line, while the limits of agreement ($\bar{x} \pm 1.96\sigma_X$) are depicted in red

R software v3.3.2. The one-way random effects ICC(ρ) obtained is 0.996 and its 95% confidence intervals (CI) are 0.984–0.999. According to Prieto et al. (1998), ICC(ρ) values higher than 0.9 reflect excellent reliability. In order to support this findings, a Bland-Altmann graphical analysis has been performed. It shows the differences between the measurements of the two systems against their averages, thus helping to better understand the agreement between both methods (Myles and Cui 2007). The graphical analysis (Fig. 8) shows that the scattered distribution of the differences between both methods entirely falls within the 95% CI, thus not suggesting the presence of relevant disagreement. Although the results of the study are promising, a study including higher number of participants and different measurements would be required to further confirm this findings.

Another goal of this evaluation is to assess the usability and interest of SPIRA according to the expert's opinion. After the realization of the study, the physical therapists were asked to provide their impressions regarding the use of SPIRA. First of all, they emphasized the large amount of time saved when using this system. Although the performance of the test has the same time consumption for both offline video analysis and SPIRA, the angle is computed automatically with the latter tool, thus removing completely the offline analysis stage. This stage comprises the insertion of the video sequences into the analysis software, the search of a particular time instant where the position of the subject is relevant, and the manual placement of the markers and lines to compose the angle. It can last up to ten minutes per subject. Moreover, the experts experienced more reliability when using SPIRA, since the whole evolution of the angle during the test is recorded, instead of freezing the video at a discrete time point and estimating the angle. For example, during the SLL test, the angle is usually measured at the maximum knee flexing point. When using offline analysis, the point when the video is frozen depends on the subjective criteria of the user, and cannot represent precisely the maximum flexing point. The real-time representation of the angle was greatly appreciated, especially to observe the fluctuations of the measurement during the realization of the test. Finally, the therapists valued positively that all the information is automatically stored in the database and the historical data can be retrieved and displayed at any time, very useful for constructing training programs. The easiness of use of the application interface was also highlighted.

At the end of the evaluation, the experts reported that they faced some troubles when any subject was wearing clothes with reflective elements, which were nevertheless overcome after following the instructions given by the designers. They also considered it desirable to include in the application a brief users' guide for the sensor setup and the test performance. All of these valuable comments have been taken into account for future extension of this work.

5 Conclusion and future work

The assessment of lower limb injury risk have become a crucial task during recent years. In this context, the measurement of body joint angles during the execution of dynamic movements has proven to be a great indicator of injury risk. However, existing techniques and traditional procedures to measure the joint angles, suffer from diverse kinds of limitations and their resource requirements made them not practical for most clinical settings. Moreover, these techniques focus on the final result rather than analyzing the evolution of the angles during the execution of the tests. To overcome these limitations, this work presents SPIRA, an automatic 2D video analysis system aimed to support experts during the performance of functional tests. The angle measurement process involves using an infrared camera to track the position of retro-reflective markers attached to the subject's body joints and compute on-the-fly the angle value based on their position. The information is processed by a computer application that guides the expert during the execution of the tests and expedites the analysis of the results and the management of the information gathered. The SPIRA system has been validated against a 2D offline video analysis software, showing a high agreement between both systems and an excellent reliability of the measurements obtained with the proposed one. In view of the promising results of the validation, we plan to develop a longitudinal study to observe the evolution of the measurements taken by SPIRA and relate them to the injuries suffered, constructing a whole injury prevention model. Moreover, we are working on the integration of a new depth sensor with higher frame rate, and the implementation of new measurements for injury risk assessment.

Acknowledgements This work has been partially supported by the Spanish Ministry of Economy and Competitiveness (MINECO) Projects TIN2015-71873-R and TIN2015-67020-P together with the European Fund for Regional Development (FEDER). This work has also been partially supported by the UGR Research Starting Grant 2017, the FPU Spanish Grant FPU16/04376 and the Dutch UT-CTIT project HoliBehave.

References

Acevedo R, Rivera-Vega A, Miranda G, Micheo W (2014) Anterior cruciate ligament injury: identification of risk factors and prevention strategies. Curr Sports Med Rep 13(3):186–191. https://doi.org/10.1249/JSR.0000000000000053

Bailon C, Damas M, Pomares H, Banos O (2017) Automatic 2D motion capture system for joint angle measurement. Springer International Publishing, Cham, pp 71–81. https://doi.org/10.1007/978-3-319-59147-6_7

Banos O, Moral-Munoz J, Diaz-Reyes I, Arroyo-Morales M, Damas M, Herrera-Viedma E, Hong C, Lee S, Pomares H, Rojas I, Villalonga C (2015) mdurance: a novel mobile health system to support trunk

endurance assessment. Sensors 15(6):13159–13183. https://doi.org/10.3390/s150613159
Bell AL, Brand RA, Pedersen DR (1989) Prediction of hip joint centre location from external landmarks. Human Mov Sci 8(1):3–16. https://doi.org/10.1016/0167-9457(89)90020-1
Bland J, Altman D (1990) A note on the use of the intraclass correlation coefficient in the evaluation of agreement between two methods of measurement. Comput Biol Med 20(5):337–340. https://doi.org/10.1016/0010-4825(90)90013-F
Booth M, Orr R (2017) Time-loss injuries in sub-elite and emerging Rugby league players. J Sports Sci Med 16:295–301
Bort-Roig J, Gilson ND, Puig-Ribera A, Contreras RS, Trost SG (2014) Measuring and influencing physical activity with smartphone technology: a systematic review. Sports Med 44(5):671–686. https://doi.org/10.1007/s40279-014-0142-5
Bouwmans T, Porikli F, Höferlin B, Vacavant A (2015) Background modeling and foreground detection for video surveillance, 1st edn. CRC Press/Taylor and Francis Group, oCLC: 934765046
Damsted C, Larsen LH, Nielsen RO (2015) Reliability of video-based identification of footstrike pattern and video time frame at initial contact in recreational runners. Gait Posture 42(1):32–35. https://doi.org/10.1016/j.gaitpost.2015.01.029
Davoody N, Hagglund M (2016) Care professionals' perceived usefulness of ehealth for post-discharge stroke patients. Stud Health Technol Inf 228:589–593. https://doi.org/10.3233/978-1-61499-678-1-589
DiCesare CA, Bates NA, Meyer GD, Hewett TE (2014) The validity of 2-dimensional measurement of trunk angle during dynamic tasks. Int J Sports Phys Ther 9(4):420–427
EmguCV (2017) EmguCV library. http://www.emgu.com/wiki/index.php/. Accessed 09 Oct 2017
Feller J, Webster KE (2013) Return to sport following anterior cruciate ligament reconstruction. International Orthopaedics 37(2):285–290. https://doi.org/10.1007/s00264-012-1690-7
van Gent RN, Siem D, van Middelkoop M, van Os AG, Bierma-Zeinstra SMA, Koes BW (2007) Incidence and determinants of lower extremity running injuries in long distance runners: a systematic review. Br J Sports Med 41(8):469–480. https://doi.org/10.1136/bjsm.2006.033548
Guerra-Filho GB (2005) Optical motion capture: theory and implementation. J Theor Appl Inf (RITA) 12(2):61–89
Herrington L (2014) Knee valgus angle during single leg squat and landing in patellofemoral pain patients and controls. KNEE 21(2):514–517. https://doi.org/10.1016/j.knee.2013.11.011
Herrington L, Munro A (2010) Drop jump landing knee valgus angle: normative data in a physically active population. Phys Ther Sport 11(2):56–59. https://doi.org/10.1016/j.ptsp.2009.11.004
Hewett TE, Myer GD (2011) The mechanistic connection between the trunk, hip, knee, and anterior cruciate ligament injury. Exerc Sport Sci Rev 39(4):161–166. https://doi.org/10.1097/JES.0b013e3182297439
Hewett TE, Myer GD, Ford KR, Heidt Robert SJ, Colosimo AJ, McLean SG, van den Bogert AJ, Paterno MV, Succop P (2005) Biomechanical measures of neuromuscular control and valgus loading of the knee predict anterior cruciate ligament injury risk in female athletes: a prospective study. Am J Sports Med 33(4):492–501. https://doi.org/10.1177/0363546504269591
Hewett TE, Di Stasi SL, Myer GD (2013) Current concepts for injury prevention in athletes after anterior cruciate ligament reconstruction. Am J Sports Med 41(1):216–224. https://doi.org/10.1177/0363546512459638
Hootman JM, Dick R, Agel J (2007) Epidemiology of collegiate injuries for 15 sports: summary and recommendations for injury prevention initiatives. J Athl Train 42(2):311–319
Kato S, Urabe Y, Kawamura K (2008) Alignment control exercise changes lower extremity movement during stop movements in female basketball players. Knee 15(4):299–304. https://doi.org/10.1016/j.knee.2008.04.003
Kinovea Association (2017) Kinovea. http://www.kinovea.org/. Accessed 09 Oct 2017
Li L (2014) Time-of-flight camera—an introduction. Technical White Paper SLOA190B, Texas Instruments
LiveCharts (2017) LiveCharts library. https://lvcharts.net/. Accessed 09 Oct 2017
Mather RC, Koenig L, Kocher MS, Dall TM, Gallo P, Scott DJ, Bach BR, Spindler KP (2013) Societal and economic impact of anterior cruciate ligament tears. J Bone Joint Surg Am 95(19):1751–1759. https://doi.org/10.2106/JBJS.L.01705
Microsoft (2014a) Kinect API. https://msdn.microsoft.com/en-us/library/dn782033.aspx
Microsoft (2014b) Kinect for windows v2. https://developer.microsoft.com/es-es/windows/kinect/develop/
Microsoft (2017a) .NET Framework. https://www.microsoft.com/net
Microsoft (2017b) Windows presentation foundation (WPF). https://docs.microsoft.com/en-us/dotnet/framework/wpf/
Microsoft (2017c) XAML Overview. https://docs.microsoft.com/en-us/dotnet/framework/wpf/advanced/xaml-overview-wpf
Moral-Muñoz JA, Esteban-Moreno B, Arroyo-Morales M, Cobo MJ, Herrera-Viedma E (2015) Agreement between face-to-face and free software video analysis for assessing hamstring flexibility in adolescents. J Strength Condition Res 29(9):2661–2665. https://doi.org/10.1519/JSC.0000000000000896
Müller B, Ilg W, Giese MA, Ludolph N (2017) Validation of enhanced kinect sensor based motion capturing for gait assessment. PLoS One. https://doi.org/10.1371/journal.pone.0175813
Munro AG (2013) The use of two-dimensional motion analysis and functional performance tests for assessment of knee injury risk behaviours in athletes. PhD thesis, University of Salford, Salford, UK
Munro AG, Herrington L, Carolan M (2012) Reliability of 2-dimensional video assessment of frontal-plane dynamic knee valgus during common athletic screening tasks. J Sport Rehabilit 21(1):7–11
Myles PS, Cui J (2007) Using the Bland–Altman method to measure agreement with repeated measures. Br J Anaesth 99(3):309–311. https://doi.org/10.1093/bja/aem214
Northern Digital Inc (2017) Optotrak certus. http://www.ndigital.com/msci/products/optotrak-certus
O'Connor S, McCaffrey N, Whyte EF, Moran KA (2017) Epidemiology of injury in male collegiate gaelic footballers in one season. Scand J Med Sci Sports 27(10):1136–1142. https://doi.org/10.1111/sms.12733
Olugbara OO, Adetiba E, Oyewole SA (2015) Pixel intensity clustering algorithm for multilevel image segmentation. Math Probl Eng 649802:19. https://doi.org/10.1155/2015/649802
Patro SGK, Sahu KK (2015) Normalization: a preprocessing stage. CoRR abs/1503.06462
Piccardi M (2004) Background subtraction techniques: a review. In: Systems, man and cybernetics, 2004 IEEE international conference on, IEEE, vol 4, pp 3099–3104
van Poppel D, Scholten-Peeters GGM, van Middelkoop M, Verhagen AP (2014) Prevalence, incidence and course of lower extremity injuries in runners during a 12-month follow-up period. Scand J Med Sci Sports 24(6):943–949. https://doi.org/10.1111/sms.12110
Prieto L, Lamarca R, Casado A (1998) La evaluación de la fiabilidad en las observaciones clínicas: el coeficiente de correlación intraclase. Med Clin 110(4):142–145
Sarbolandi H, Lefloch D, Kolb A (2015) Kinect range sensing: structured-light versus time-of-flight kinect. Comput Vis Image Understand 139:1–20. https://doi.org/10.1016/j.cviu.2015.05.006
Shapiro LG, Stockman GC (2002) Computer Vision, Prentice Hall, chap Binary Image Analysis, pp 69–73

SQLite (2017) SQLite engine. http://www.sqlite.org/

Stickler L, Finley M, Gulgin H (2015) Relationship between hip and core strength and frontal plane alignment during a single leg squat. Phys Ther Sport 16(1):66–71. https://doi.org/10.1016/j.ptsp.2014.05.002

Szeliski R (2011) Computer vision: algorithms and applications. Texts in computer science, Springer, London Dordrecht Heidelberg New York, oCLC: 845585642

Vicon Motion Systems Ltd (2002) Essential of motion capture. Tech. rep

Vicon Motion Systems Ltd (2017) Vicon cameras. https://www.vicon.com

Willson JD, Davis IS (2008) Utility of the frontal plane projection angle in females with patellofemoral pain. J Orthopaed Sports Phys Ther 38(10):606–615. https://doi.org/10.2519/jospt.2008.2706

Willson JD, Ireland ML, Davis I (2006) Core strength and lower extremity alignment during single leg squats. Med Sci Sports Exerc 38(5):945–952. https://doi.org/10.1249/01.mss.0000218140.05074.fa

Wyndow N, De Jong A, Rial K, Tucker K, Collins N, Vicenzino B, Russell T, Crossley K (2016) The relationship of foot and ankle mobility to the frontal plane projection angle in asymptomatic adults. J Foot Ankle Res 9(1):3